

## Experimental analysis of a new high-tech method of strengthening reinforced concrete structures based on the use of metal and CFRP materials

Georgiev S.V.<sup>1</sup> , Mailyan D.R.\*<sup>1</sup> , Solovyeva A.I.<sup>1</sup> ,  
Che XiangYu<sup>1</sup> , Kiiamova L.I.<sup>2</sup> 

<sup>1</sup> Don State Technical University, Russia,

<sup>2</sup> Moscow State University of Civil Engineering, Russia

**Abstract.** This paper presents a large-scale experimental analysis of a new high-tech method for strengthening reinforced concrete columns using metal and CFRP materials. The research is justified by evaluating existing traditional and modern methods of strengthening reinforced concrete compressed elements, identifying their main drawbacks, and taking these into account, a new strengthening method was developed. To study the large-scale effect of the new high-tech metal and composite-based strengthening method, two groups of a total of 46 reinforced concrete column samples with different flexibilities were designed and tested for central and eccentric compression until failure. The main test parameters included column flexibility, load application eccentricity, internal and external metal reinforcement, spacing, and cross-sectional area of composite strengthening. The study investigated the influence of the above-mentioned variable factors on the failure pattern, ultimate strength, peak stress, and deformation characteristics of columns strengthened with carbon fiber composite materials (CFRP). The results showed that reinforced concrete columns strengthened with CFRP, having the same dimensions and tested under the same load application eccentricities, demonstrated different increases in ultimate strength compared to unstrengthened columns. Peak stress increased with an increase in the cross-sectional area of metal reinforcement and decreased with an increase in the distance between composite stirrups. Ultimate axial strains of strengthened samples increased with a decrease in the distance between composite stirrups. The difference in the cross-sectional area of composite strengthening did not have a significant impact on the load-bearing capacity and ultimate strains of reinforced concrete strengthened structures.

**Keywords:** heavy concrete, reinforced concrete, test, column, metal, composite material, CFRP, FRP

**Please cite this article as:** Georgiev S.V., Mailyan D.R., Solovyeva A.I., Che XiangYu, Kiiamova L.I. Experimental analysis of a new high-tech method of strengthening reinforced concrete structures based on the use of metal and CFRP materials. *Construction Materials and Products*. 2025. 8 (6). 9. DOI: 10.58224/2618-7183-2025-8-6-9

\*Corresponding author E-mail: [dmailyan868@mail.ru](mailto:dmailyan868@mail.ru)

## 1. INTRODUCTION

Composite materials based on carbon fiber-reinforced polymer (CFRP) offer key advantages such as low weight, high strength, corrosion resistance, and long-term durability, leading to their increasing adoption in civil engineering applications. The technique of strengthening axially loaded reinforced concrete members using CFRP jackets or bandages has been demonstrated in study [1] to be highly effective. Based on experimental data from foreign studies and a large number of tests on compressed members with circular and rectangular cross-sections, numerous models of strength and deformability have been developed. Structural relationships for concrete columns with circular cross-sections are examined in studies [2–9], while those for reinforced concrete columns [10–12] with rectangular cross-sections are covered in studies [13–16].

However, existing experimental studies have demonstrated insufficient effectiveness of composite strengthening for slender eccentrically loaded reinforced concrete members [17], where the vulnerable zone is the tensile face of the eccentrically compressed, strengthened specimen. Composite material placed in the compression zone and subjected to axial compression is ineffective [18]. In turn, the conventional and most widely used strengthening method—steel jacketing—is effective only for short eccentrically loaded columns subjected to small load eccentricities. Practical experience has shown that the majority of structural elements used in construction are subjected to eccentric compression [19, 20] and typically exhibit relatively high slenderness ratios. Under such loading conditions, jacket-type strengthening of load-bearing members is impractical [21]. Instead of transverse composite confinement, specialized laminates or carbon fiber fabrics are bonded to the tensile zone of reinforced concrete members. Reinforced concrete columns subjected to large load eccentricities behave according to a flexural (beam-like) scheme; therefore, enhancing their strength depends not only on increasing the tensile capacity of the tension zone but also on improving the load-carrying capacity of the concrete in the compression zone.

In view of the current state of both domestic and international research, the authors have developed a novel strengthening method that combines steel and carbon fiber-reinforced polymer (CFRP) composite materials. They tested 46 columns strengthened with this hybrid steel–CFRP system under both concentric and eccentric compression. The authors analyzed the influence of various controllable parameters and provided experimental data for engineering practice.

## 2. METHODS AND MATERIALS

The experimental program comprised 46 concrete and reinforced concrete columns.

The experimental phase can be conditionally divided into two stages.

The first stage involved testing two series of specimens comprising 13 and 12 columns, respectively. Both series had identical overall dimensions but differed in the presence of internal reinforcement (Fig. 1).

The second stage also included two series of columns, with 11 and 10 specimens per series, respectively (Figs. 2 and 3). Within this stage, the columns of one series differed from those of the other in slenderness ratio. This division was implemented to evaluate the effectiveness of the hybrid steel–composite strengthening for members with low slenderness ( $\lambda_h = 10$ ) and high slenderness ( $\lambda_h = 20$ ). In this stage, all test specimens within each series were subjected to loading at three eccentricities:  $e_0 = 0$ ,  $e_0 = 2$  cm, and  $e_0 = 4$  cm. This approach was adopted to assess the performance of the hybrid steel–composite strengthening system under concentric compression, eccentric compression with a small eccentricity (within the core of the cross-section), and eccentric compression with a large eccentricity (outside the core of the cross-section).

Thus, the scope of the study consisted in evaluating the effectiveness of the hybrid steel–composite strengthening system for plain concrete specimens, reinforced concrete specimens with slenderness ratios  $\lambda_h = 4, 10$ , and  $20$ , and under various load eccentricities. The latter enabled the determination of the stress–strain state of columns under complex stress conditions.

Given the novelty of the proposed hybrid steel–composite strengthening method—which has no known analogues—the authors obtained an invention patent [22].

In each series across both experimental stages, three strengthening parameters were varied: the type of external steel reinforcement, the thickness of the composite hoops (wraps), and their spacing (pitch).

The experimental program and strengthening configurations are presented in Figs. 1–3.

All test specimens were assigned identification codes. The coding system for the experimental specimens is provided below:

1) Coding system for Stage I columns:

**The first** letter of the code (a capital letter of the English alphabet) denotes a column with dimensions of 60×15×15 cm. The letter «P» denotes columns without an internal frame; «K» denotes columns with a reinforcing cage.

**The second** letter (also a capital English letter) indicates the presence or absence of composite strengthening. The letter «U» - denotes strengthened with composite material, «E» – denotes reference columns without composite strengthening, **The presence of subscript** «1» or «2» next to the code indicates the number of the twin test specimen.

**The third** letters of the code, also capital letters of the English alphabet, denote:

— The letter «M» – indicates steel angles bonded to all four corners of the column. **Subscript** «1» denotes angle size 40×40 mm; **subscript** «2» denotes 25×25 mm. **Superscript** «2» (if present) indicates double-layer angles (two angles stacked on each corner).

— The letter «S» – denotes column corner rounding achieved by shotcreting, converting the original square cross-section into a circular one;

**The fourth** letter «X» signifies transverse reinforcement using composite hoops (wraps). Indices specify: **superscript** number of hoop layers – «1» for a single layer, «2» for two layers. **Subscript** hoop width – «1» for 25 mm, «2» for 50 mm, and «3» for 75 mm.

**The fifth** letter of the code, also a capital letter of the English alphabet – «H» – indicates the presence of special composite patches with fibers oriented transversely, bonded to the column corners in three layers. **The superscript** «3» denotes the number of patch layers.



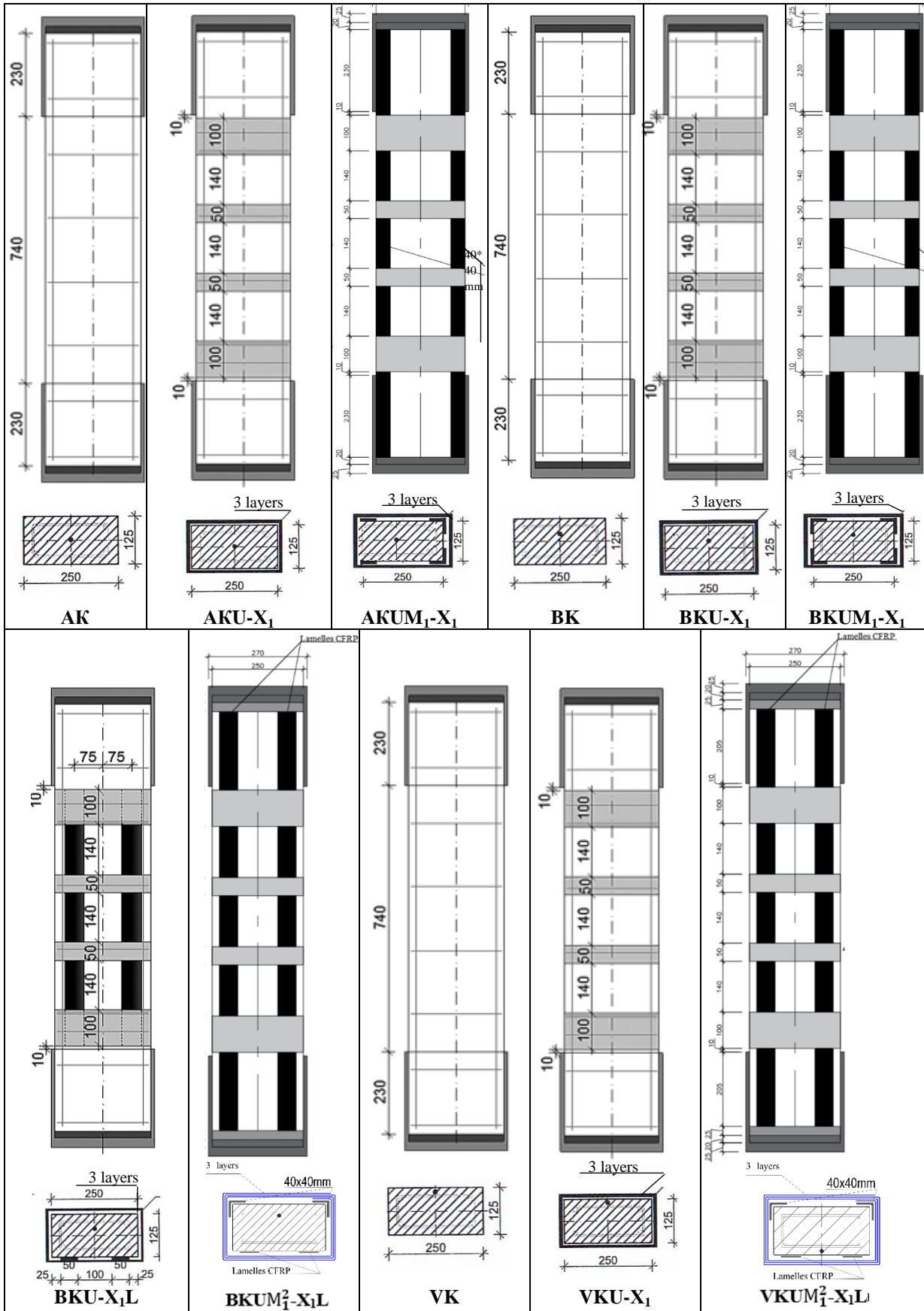


**Fig. 2.** Experimental program for Stage II, Series I columns with cross-section 250 × 125 mm (height) and length of 1200 mm.

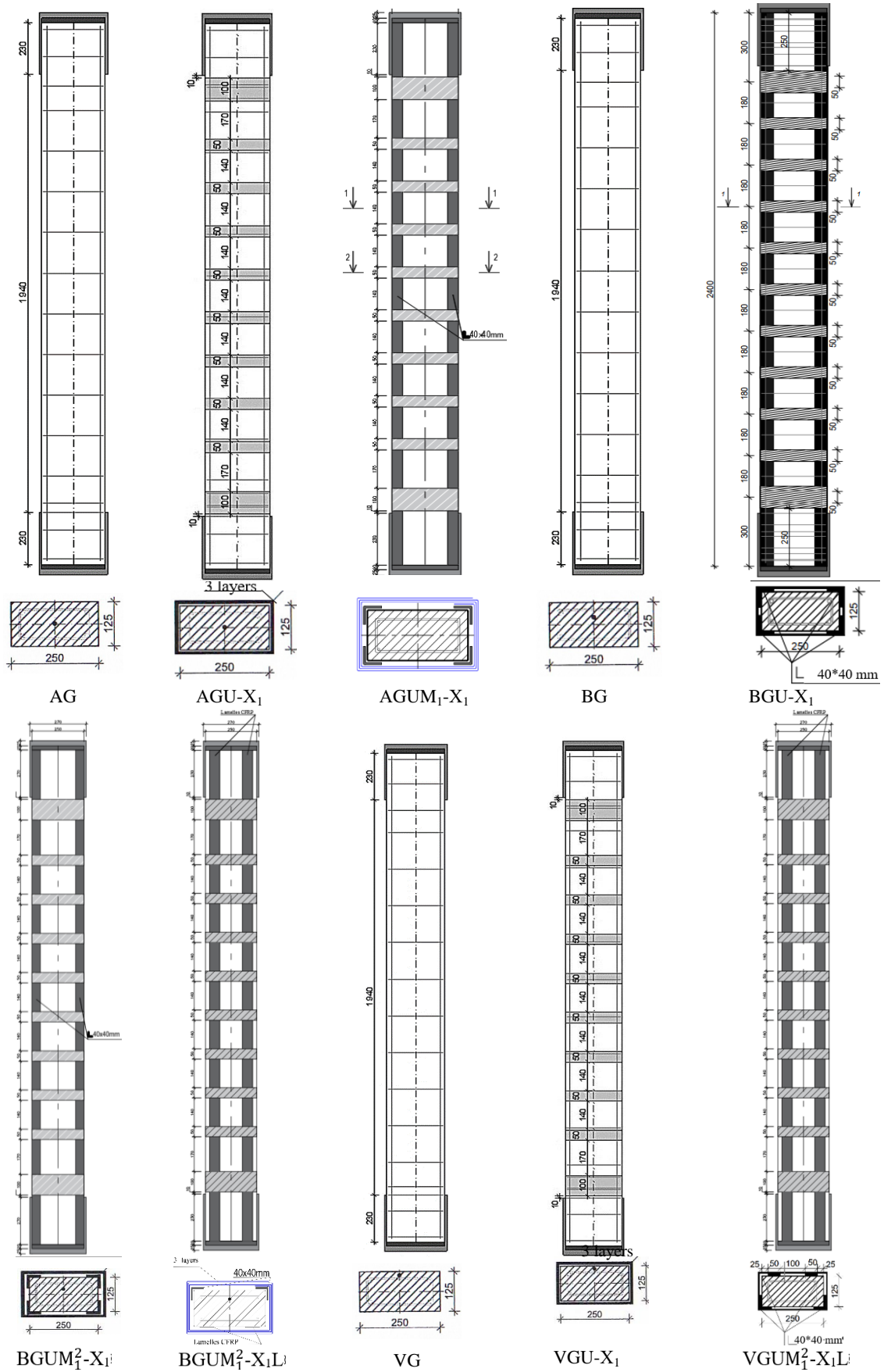


**Fig. 3.** Experimental program for Stage II, Series II columns with cross-section 250 × 125 mm (height) and length of 2400 mm.

## 2) Coding system for Stage II columns:

Applies to reinforced concrete columns with a cross-section of  $250 \times 125$  mm (height) and lengths of 1200 mm and 2400 mm.

**The first** letter of the code (a capital letter of the English alphabet) – denotes the axial eccentricity ( $e_0$ ):

- «A» – concentrically-compressed columns,  $e_0=0$ .
- «B» – columns tested with an eccentricity of  $e_0=2$ cm;
- «V» – columns tested with an eccentricity of  $e_0=4$ cm.

**The second** letter (English alphabet) denotes the type of reference column – for short columns «K» or «G» for slender columns.

**The third** letter of the english alphabet «U» indicates that the specimen is strengthened.

**The fourth** letter of the english alphabet «M» signifies steel angles bonded to all four corners of the column. **The subscript** denotes the size of the equal-leg steel angle: «1» for  $40 \times 40$  mm and «2» for  $25 \times 25$  mm. **Superscript** «2» (if present) indicates that only two steel angles are used, positioned on the compression face of the column.

**The fifth** symbol «X<sub>1</sub>» (letter of the english alphabet with numeric subscript) denotes transverse reinforcement using composite hoops (wraps) 50 mm wide, spaced at 190 mm on center.

**The sixth** letter (Latin alphabet) indicates the presence of longitudinal CFRP strengthening:

– «L» denotes the use of CFRP laminates (strips) 50 mm wide and 1,2 mm thick, applied in a quantity of two strips.

### Material Properties

**Materials for Concrete Production.** The primary materials used to fabricate the test specimens included concrete, steel reinforcement, structural steel sections, carbon fiber fabric, carbon fiber laminates, and an adhesive system employed for bonding the external strengthening layers. Detailed information regarding the concrete mix design and the properties of constituent materials—such as sand, cement, and coarse aggregate—as well as the characteristics of both steel and composite reinforcement, are provided in a previously published paper from this research study [23].

Only the key properties are presented below.

Heavyweight concrete was used for specimen fabrication, with its compressive strength specified in Tables 1 and Tables 2.

For Stage I specimens, longitudinal reinforcement of grade A500 with a diameter of 10 mm was used, while for Stage II specimens, longitudinal reinforcement of the same grade but with a diameter of 12 mm was employed. Smooth transverse reinforcement of grade B500 was used in both experimental stages.

Reinforcement details for Stage II columns with lengths of 1200 mm and 2400 mm are shown in Fig. 4.

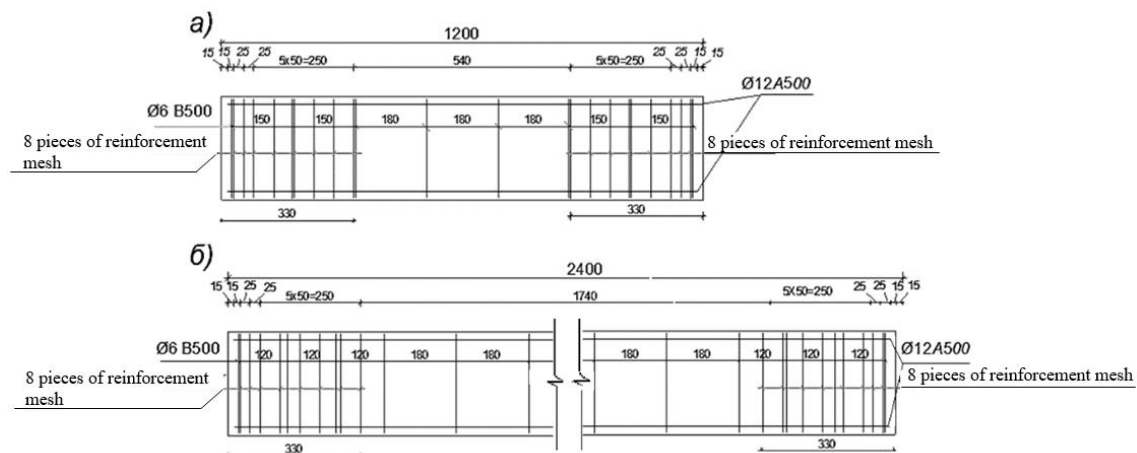


**Fig. 4.** Longitudinal and transverse reinforcement layout of columns: a) rack  $250 \times 125 \times 1200$  mm; b) rack with a section of  $250 \times 125 \times 2400$  mm;

Carbon fiber fabric was used as the composite material, with a tensile strength of the carbon fibers equal to 4900 MPa. According to the manufacturer's data, the elastic modulus of the carbon fabric was 300 GPa.

**Fabrication and Strengthening Procedure for Columns.** All columns from both Stage I and Stage II were cast in the university laboratory. Each concreting operation was accompanied by the production of control specimens—specifically, 10×10 cm and 15×15 cm cubes, twelve in total. These cubes were tested on the same day as the first specimens of the corresponding series to determine the concrete compressive strength.

Strengthening of the test specimens was carried out in two stages.

The first stage involved preparatory works and bonding steel angles to the column corners. Prior to adhesive application, column surfaces were ground with abrasive machines until the coarse aggregate (gravel) was exposed, then thoroughly cleaned of dust and primed with specialized primer mixtures. The steel angles were bonded using an epoxy adhesive—the same adhesive employed for bonding carbon fiber laminates.

The second strengthening stage consisted of applying composite hoops (wraps) and carbon fiber laminates.

**Test Methodology for Experimental Specimens.** Column testing was carried out on two hydraulic presses specially equipped for instrumentation. Stage I specimens were tested on a 2500 kN press, while Stage II columns were tested on a 5000 kN press (Fig. 5).

Prior to each test, instrumentation was installed on every specimen to measure concrete and composite material strains, as well as deflections (for Stage II columns). Electronic displacement transducers with a resolution of 0.001 mm were used to monitor concrete strain. These transducers were mounted at mid-height of the specimen on all four faces, with a gauge length of 200 mm for Stage I and 300 mm for Stage II.

Electrical resistance strain gauges (strain gauges) were employed to capture local deformations. They were bonded directly onto both the concrete surface and the composite strengthening materials. The primary purpose of using strain gauges was to monitor localized material strains during loading.

Deflection measurements were performed only during Stage II. To determine net lateral deflections, three dial gauges (deflectometers) were installed—at the top, mid-height, and bottom of each column.



**Fig. 5.** Test setup configuration for 2500 kN and 5000 kN presses.

Testing was carried out under incrementally increasing load up to failure. Each load step corresponded to approximately one-tenth of the anticipated ultimate load and was held for 10 to 15 minutes.

### 3. RESULTS AND DISCUSSION

**Failure Mode.**

Specimens with different strengthening configurations failed in a similar manner under identical loading conditions. During the initial loading stages, no visible changes were observed in the concrete or strengthening materials. As the load increased, cracking sounds were heard in the composite hoops, although no visible damage or delamination occurred. At load levels of approximately 80% of the ultimate failure load, concrete buckling between the hoops was observed. Failure was accompanied by a sudden, explosive sound, and in most cases, one of the hoops—typically located near the mid-height of the specimen—ruptured. The concrete immediately above and below the ruptured hoop crushed. The steel angles beneath the hoop bent outward, yet remained bonded to the concrete in the regions near the supports and under other intact hoops.

A plain concrete column strengthened only with steel angles (without composite hoops) failed in a classical manner, similar to an unstrengthened specimen.

No significant difference in failure mode was observed between plain concrete and reinforced concrete columns tested in Stage I.

Several columns from Series II of Stage I, which had undergone preliminary section rounding (shotcreting to convert square sections into circular ones), failed gradually, with localized rupture of the transverse external reinforcement. The failure mode of these rounded columns is described in detail in a previously published paper of this study [23].

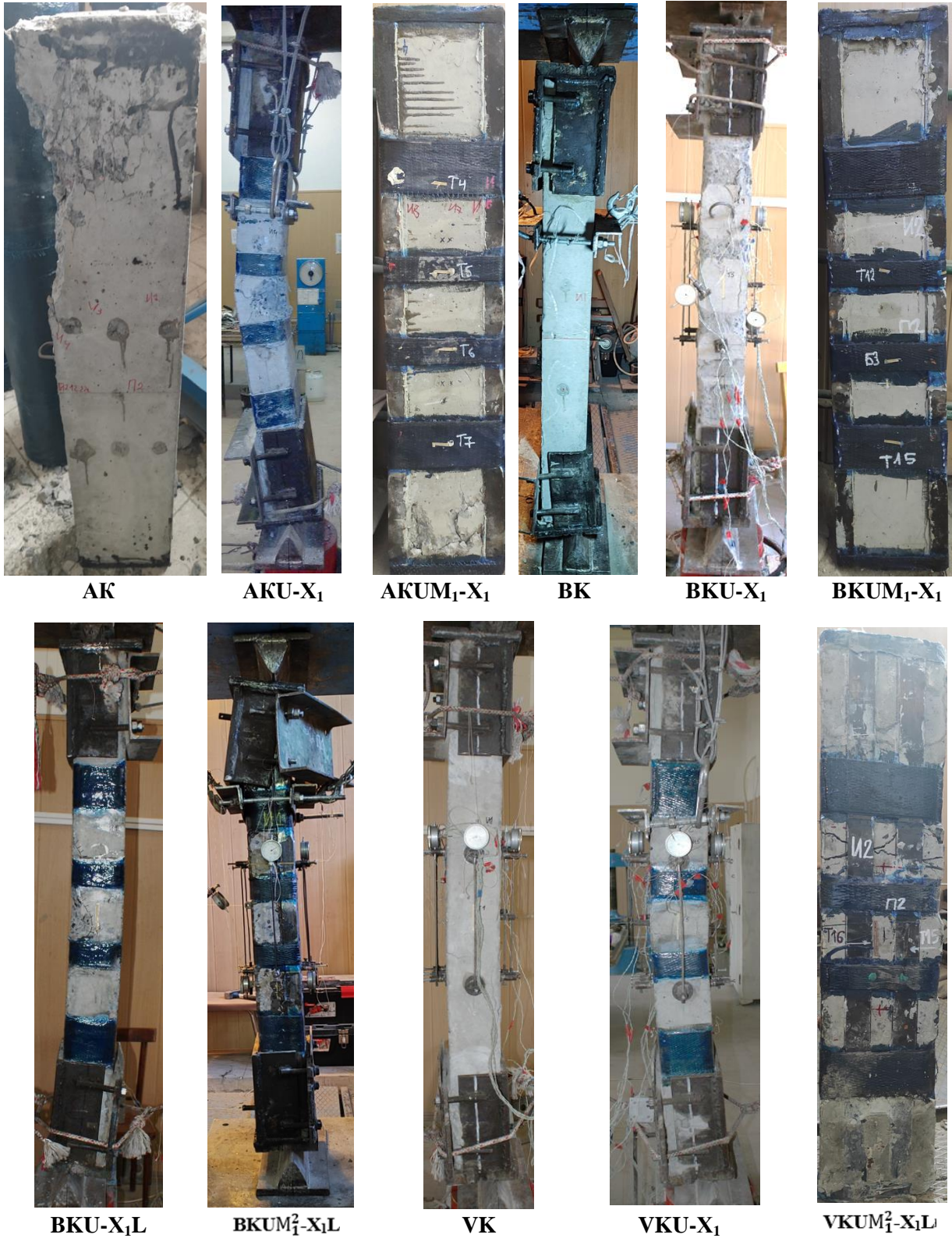
The failure mode of Stage II columns depended on the magnitude of the load eccentricity. Centrally loaded columns failed in a relatively ductile manner: the concrete between the hoops began to spall, accompanied by a gradual load drop. At failure, the concrete between the hoops—primarily near mid-height—crushed, and both the internal steel reinforcement and external steel angles exhibited outward buckling.

Eccentrically loaded columns primarily failed due to crushing of the concrete in the compression zone. At failure, these specimens exhibited lateral buckling, crushing of the compressed concrete zone, and visible cracking on the tension face.

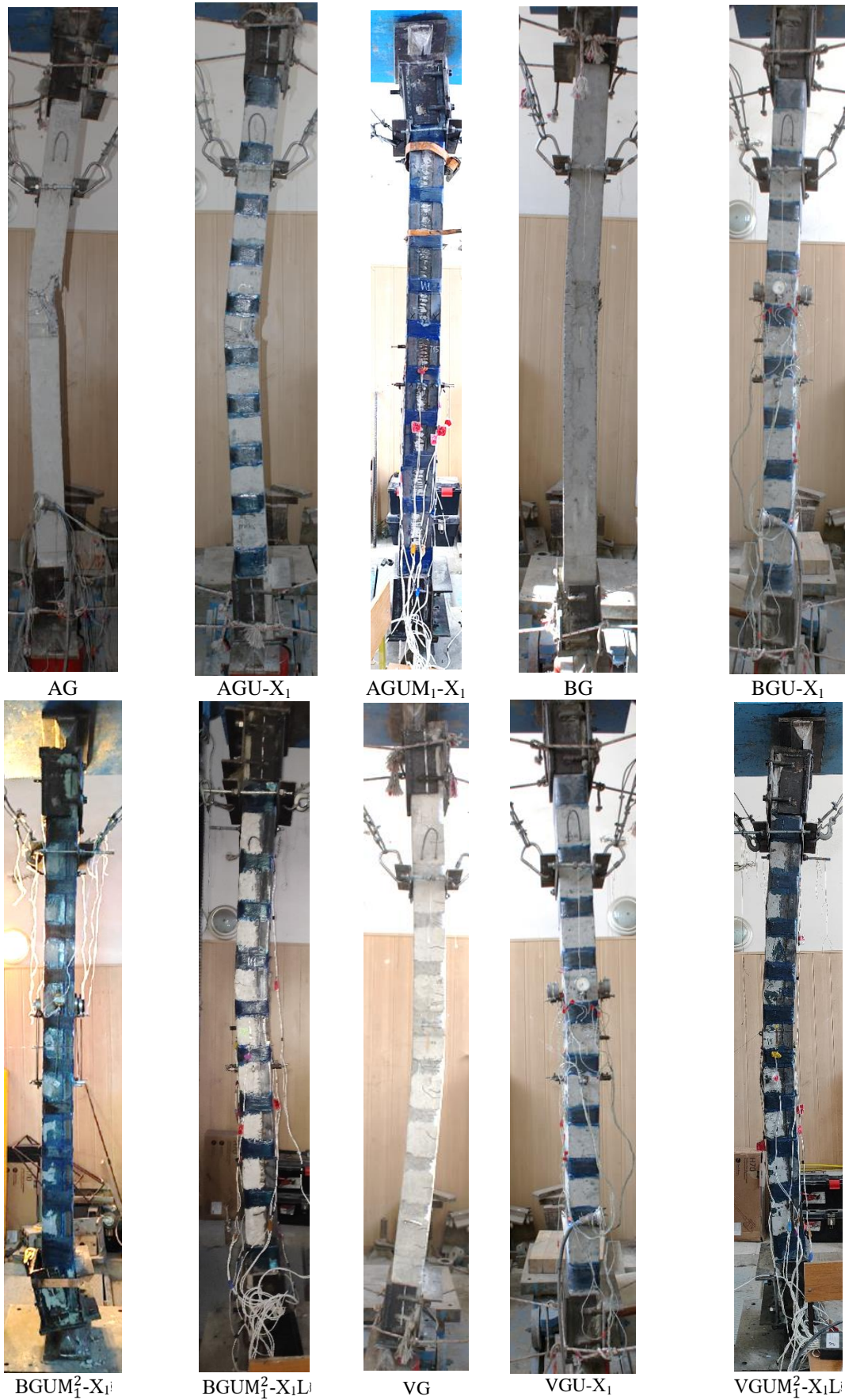
The behavior and failure modes of all test specimens under various strengthening configurations are described in the text and illustrated in Figs. 6-8.



Fig. 6. Failure mode of columns in Stage I, Series I and II of the experimental program.



**Fig. 7.** Failure mode of columns in Stage II, Series I of the experimental program (columns with cross-section 250 × 125 mm (height) and length of 1200 mm).



**Fig. 8.** Failure mode of columns in Stage II, Series II of the experimental program (columns with cross-section  $250 \times 125$  mm (height) and length of 2400 mm).

Test results for all concrete and reinforced concrete columns are presented in Tables 1 and 2.

As shown in Table 1, strengthened columns from Stage I of the study exhibited an increase in load-carrying capacity ranging from 10% to 48%. The minimum strengthening effect was observed for columns reinforced with 25×25 mm steel angles. The maximum strength gain—approximately 50%—was achieved in columns strengthened with 40×40 mm steel angles and two layers of 50 mm wide carbon fiber fabric hoops. Columns strengthened solely with externally bonded steel angles (without composite hoops) demonstrated no increase in strength. Columns strengthened by preliminary section rounding followed by composite jacketing exhibited a strength increase exceeding 300%.

**Table 1.** Results of Stage I tests for Series I and II columns.

Serial number	Column designation	$\bar{R}_b$ МПа	Column strength, кН		Strengthening coefficient based on direct comparison, $k_f$	Strengthening coefficient, accounting for the adjusted concrete strength, $k'_f$
			$N_{s,ult}$	$N_{f,ult}$		
1	2	3	4		5	6
1.	PE <sub>1</sub>	41,8	700	701,1	1,00	1,00
2.	PE <sub>2</sub>	41,8	702,5			
3.	PUM <sub>1</sub>	44,6	737,5		1,05	0,986
4.	PUM <sub>1</sub> -X <sub>1</sub> <sup>1</sup>	41,8	812,5		1,16	1,16
5.	PUM <sub>1</sub> -X <sub>1</sub> <sup>2</sup>	44,6	952,5		1,36	1,27
6.	PUM <sub>1</sub> -X <sub>2</sub> <sup>2</sup>	44,6	1100,0		1,57	1,47
7.	PUM <sub>1</sub> -X <sub>2</sub> <sup>2</sup> H <sup>2</sup>	41,8	1015,0		1,45	1,45
8.	PUM <sub>2</sub> -X <sub>1</sub> <sup>1</sup>	41,8	800,0		1,14	1,14
9.	PUM <sub>2</sub> -X <sub>2</sub> <sup>1</sup>	46,0	810,0		1,16	1,05
10.	PUM <sub>2</sub> -X <sub>3</sub> <sup>1</sup>	41,8	900,0		1,28	1,28
11.	PUM <sub>2</sub> -X <sub>1</sub> <sup>2</sup>	46,0	852,5		1,22	1,11
12.	PUM <sub>2</sub> -X <sub>2</sub> <sup>2</sup>	46,0	1072,5		1,53	1,39
13.	PUM <sub>2</sub> <sup>2</sup> -X <sub>2</sub> <sup>1</sup>	41,8	900,0		1,28	1,28
14.	KE <sub>1</sub>	46,0	962,5	959,0	1,00	1,00
15.	KE <sub>2</sub>	46,0	955,5			
16.	KUM <sub>2</sub> -X <sub>1</sub> <sup>2</sup>	44,6	1125,0		1,25	1,29
17.	KUM <sub>2</sub> -X <sub>2</sub> <sup>2</sup>	44,6	1200,0		1,25	1,29
18.	KUM <sub>1</sub>	44,6	712,5		0,97	1,00
19.	KUM <sub>1</sub> -X <sub>1</sub> <sup>2</sup>	44,6	1100,0		1,14	1,14
20.	KUM <sub>1</sub> -X <sub>2</sub> <sup>2</sup>	46,0	1200,0		1,25	1,25
21.	KES	46,0	960,0		1,00	1,00
22.	KU	44,6	1190,0		1,24	1,28
23.	KUN	44,6	1400,0		1,46	1,51
24.	PUS	46,0	2200,0		3,14	2,70
25.	KUS	46,0	2500,0		2,61	2,61

Note: Formulas for calculating strengthening coefficients – based on direct comparison of the strength of reference and strengthened specimens, and accounting for the normalized (adjusted) concrete compressive strength

$$k_f = N_{f,ult}/N_{s,ult} ; k'_f = N_{f,ult}/N_{s,ult} \cdot \bar{R}_s^{exp} / \bar{R}_f^{exp}$$

**Table 2.** Results of Stage II tests for Series I and II specimens.

Serial number	Column designation	$R_b$ МПа	Column strength, $\kappa H$ $N_{s,ult}, N_{f,ult} \kappa H$	Strengthening coefficient based on direct comparison, $k_f$	Strengthening coefficient, accounting for the adjusted concrete strength, $k'_f$
1	2	3	4	5	6
1.	AK	28,0	1340,0	1,00	1,00
2.	AKU-X <sub>1</sub>	23,2	1200,0	0,90	1,08
3.	AKUM <sub>1</sub> -X <sub>1</sub>	23,2	1486,0	1,11	1,34
4.	BK	20,3	834,0	1,00	1,00
5.	BKU-X <sub>1</sub>	20,3	785,0	0,94	0,94
6.	BKUM <sub>1</sub> -X <sub>1</sub>	20,3	1104,1	1,32	1,32
7.	BKU-X <sub>1</sub> L	20,3	710,0	0,9	0,90
8.	BKUM <sub>1</sub> <sup>2</sup> -X <sub>1</sub> L	20,3	950,0	1,14	1,14
9.	VK	42,6	430,0	1,00	1,00
10.	VKU-X <sub>1</sub>	42,6	489,0	1,14	1,14
11.	VKUM <sub>1</sub> <sup>2</sup> -X <sub>1</sub> L	28,0	768,2	1,79	2,74
12.	AG	39,2	800,0	1,00	1,00
13.	AGU-X <sub>1</sub>	38,4	880,0	1,10	1,12
14.	AGUM <sub>1</sub> -X <sub>1</sub>	34,0	1506,0	1,88	2,17
15.	BG	30,6	415,0	1,00	1,00
16.	BGU-X <sub>1</sub>	30,0	404,5	1,00	0,97
17.	BGUM <sub>1</sub> <sup>2</sup> -X <sub>1</sub>	34,2	1010,0	2,43	2,18
18.	BGUM <sub>1</sub> <sup>2</sup> -X <sub>1</sub> L	31,3	850,0	2,05	2,00
19.	VG	45,2	250,0	1,00	1,00
20.	VGU-X <sub>1</sub>	45,2	290,0	1,16	1,16
21.	VGUM <sub>1</sub> <sup>2</sup> -X <sub>1</sub> L	34,2	603,4	2,41	3,19

Stage II of the study involved testing full-scale reinforced concrete columns with two different slenderness ratios. Although this stage comprised two specimen series, it is convenient to analyze the results according to the load eccentricity.

For concentrically loaded columns, the strengthening method employed consisted of a single type of composite hoop spaced at 190 mm and four steel angles (40 × 40 mm) bonded to the column corners. Columns strengthened with hoops only exhibited a negligible strength increase—within typical experimental scatter—indicating that, in this configuration, the hoops primarily acted as anchorage devices. Specimens strengthened with both hoops and steel angles demonstrated strength gains of 33% and 119% for columns with slenderness ratios  $\lambda_h = 10$  and  $\lambda_h = 20$ , respectively. For eccentrically loaded columns with small load eccentricity, two strengthening approaches were investigated: bonding four steel angles to the specimen, and applying CFRP laminates to the less-compressed or tensile face of the column.

The highest effectiveness was achieved with the four steel angles, yielding a 30% strength increase. In contrast, specimens strengthened with laminates instead of angles showed only a 10% strength gain. This suggests that the less-compressed face essentially lies near the neutral axis under such loading conditions.

The most pronounced effectiveness of the hybrid steel–composite strengthening was observed in slender eccentrically loaded columns subjected to large load eccentricity. Columns strengthened with composite material alone again showed virtually no strength enhancement (near-zero strengthening coefficient). However, when steel angles were applied to the compression zone and CFRP laminates to the tension zone, strength increases of 174% and 222% were achieved.

### Stress «Strain Curves».

Stress–strain curves for concrete and reinforced concrete columns with slenderness ratio  $\lambda_h = 4$ , strengthened with hybrid steel–composite systems, are presented in Figs. 9–11. For clarity and to avoid overcrowding the graphs, all columns were numbered consecutively from 1 to 24. Each number corresponds to a specific column designation (code). The column numbers along with their respective codes are listed below.

Column numbers and corresponding designations:

1- PE<sub>1</sub>; 2-PE<sub>2</sub>; 3- PUM<sub>1</sub>; 4-PUM<sub>1</sub>-X<sub>2</sub><sup>1</sup>; 5-PUM<sub>1</sub>-X<sub>1</sub><sup>2</sup>; 6-PUM<sub>1</sub>-X<sub>2</sub><sup>2</sup>; 7-PUM<sub>1</sub>-X<sub>2</sub><sup>2</sup>H<sup>2</sup>; 8-PUM<sub>2</sub>-X<sub>1</sub><sup>1</sup>; 9-PUM<sub>2</sub>-X<sub>2</sub><sup>1</sup>; 10-PUM<sub>2</sub>-X<sub>3</sub><sup>1</sup>; 11-PUM<sub>2</sub>-X<sub>1</sub><sup>2</sup>; 12-PUM<sub>2</sub>-X<sub>2</sub><sup>2</sup>; 13-PUM<sub>2</sub><sup>2</sup>-X<sub>2</sub><sup>1</sup>; 14-KE<sub>1</sub>; 15-KE<sub>2</sub>; 16-KUM<sub>2</sub>-X<sub>1</sub><sup>2</sup>; 17-KUM<sub>2</sub>-X<sub>2</sub><sup>2</sup>; 18-KUM<sub>1</sub>; 19-KUM<sub>1</sub>-X<sub>1</sub><sup>2</sup>; 20-KUM<sub>1</sub>-X<sub>2</sub><sup>2</sup>; 21-KES; 22-KU; 23-KUN; 24-KUS.

The relationship between concrete strain and load level—considering variations in strengthening configuration, column slenderness ( $\lambda_h=10$ ,  $\lambda_h=20$ ), and load eccentricity ( $e_0=0$ ;  $e_0=2\text{cm}$ ;  $e_0=4\text{cm}$ ), — was evaluated using the graphs presented in Figs. 12–17, these figures compare experimental values of concrete strains: compressive strain –  $\varepsilon_b$  versus tensile strain–  $\varepsilon_{bt}$ , or strains on the more and less compressed faces of the concrete section–  $\varepsilon_{b1}$  and  $\varepsilon_{b2}$ . Concrete deformability was also assessed by directly comparing the measured strains of strengthened specimens with those of reference (unstrengthened) specimens.

The reported strain values represent the average of strains measured on all four faces of each test specimen. This approach eliminated the influence of stress eccentricity caused by unintended (accidental) load eccentricity during testing.

### Stress–Strain State of Compressed Columns with Slenderness $\lambda_h = 4$ (Stage I of the Study).

Figure 9 presents the stress-strain curves (concrete strain vs. load) for plain concrete columns tested during Stage I. An analysis of the curves in Fig. 9 reveals the following: up to a load level of approximately 600 kN, nearly all columns exhibited similar deformation behavior. Minor differences in strain values were attributed to the presence and magnitude of accidental eccentricity, which induced non-uniform stress distribution across the column cross-sections. Reference specimens and those without transverse composite strengthening demonstrated comparable strains, ranging from  $1,5 \cdot 10^{-3}$  to  $2,0 \cdot 10^{-3}$ . The highest ultimate strains—and, correspondingly, the highest overall strength—were recorded for specimens strengthened with  $40 \times 40$  mm steel angles and 50 mm wide composite hoops, reaching  $\varepsilon_b=2,7 \cdot 10^{-3}$ .

The general development of concrete strains followed a classical pattern for both reference and strengthened columns. Most strain curves recorded at failure exhibited three distinct stages: elastic, elasto-plastic, and plastic.

Reinforced concrete columns from Series II of Stage I (Fig. 10) demonstrated the following behavior: the development of concrete strains up to failure followed a similar trend across specimens. The highest strains were observed in specimens strengthened with two layers of composite hoops, regardless of hoop width.

Figure 11 shows the strain development in columns strengthened by preliminary section rounding (via shotcreting) followed by transverse composite confinement. Up to a load level of 900 kN, all strengthened specimens exhibited similar strain behavior. The exception was Column 22, strengthened only with a mortar jacket without transverse composite reinforcement; this specimen exhibited poor composite action between the original column and the mortar jacket.

At higher load levels, specimens strengthened with a rounded-section jacket demonstrated strains exceeding the ultimate strains of reference columns by more than five times.

### Stress–Strain State of Columns with Slenderness Ratios $\lambda_h=10$ and $\lambda_h=20$ (Stage II of the Study).

Stress-strain curves for concrete were plotted separately for the compressed and tensile (or less-compressed) faces of the columns.

An analysis of concrete strain data for concentrically loaded columns with slenderness  $\lambda_h = 10$  (Fig. 12) reveals the following: reference specimens and columns strengthened only with composite hoops spaced at 140 mm exhibited nearly identical concrete strain values in both compression and tension. In contrast, the column strengthened with steel angles bonded to all four corners (specimen BKUM<sub>1</sub>-X<sub>1</sub>) demonstrated a significant increase in strength, accompanied by substantially lower concrete strains compared to the reference specimens. This indicates a high degree of composite action between the steel angles and the concrete core, resulting in enhanced load-carrying capacity and reduced deformability. A similar trend was observed for columns with slenderness  $\lambda_h = 20$  under concentric loading (Fig. 15), where ultimate strains reached  $2,5 \cdot 10^{-3}$ .

For columns with  $\lambda_h=10$  tested under a small eccentricity  $e_0=2\text{cm}$ , the reference specimen and the specimen strengthened only with hoops exhibited average concrete strains of approximately  $3,5-4,0 \cdot 10^{-3}$ . The column strengthened solely with CFRP laminates applied to the tension face (VKU-X<sub>1</sub>L) showed significantly higher strains than the reference specimen. However, at a load level of  $0.85N_{ult}$ , plastic strains began to develop in the concrete. The CFRP laminates remained essentially inactive (located near the neutral axis) until just before failure, after which they engaged abruptly and contributed to load resistance up to collapse.

Columns strengthened with hybrid steel-composite systems (BKUM<sub>1</sub>-X<sub>1</sub> и BKUM<sub>1</sub><sup>2</sup>-X<sub>1</sub>L) in the compression zone exhibited substantially lower concrete strains than the reference specimens, with maximum compressive strains not exceeding  $2,5 \cdot 10^{-3}$ . On the opposite (tensile) face, both steel angles and CFRP laminates remained near the neutral axis throughout the test until failure. For columns tested under a larger eccentricity ( $e_0 = 4 \text{ cm}$ ), the hybrid steel-composite strengthened specimen demonstrated a significant strength increase, although ultimate concrete strains were higher. Notably, at a load level of  $0.85N_{ult}$ , concrete strains already reached  $3 \cdot 10^{-3}$ . Further loading resulted in pronounced concrete creep, with a sharp increase in strain during load hold periods. A similar behavior was observed for slender  $\lambda_h = 20$  concentrically loaded columns tested at  $e_0=2 \text{ cm}$  и  $e_0=4 \text{ cm}$ , respectively.

Under concentric compression, columns with  $\lambda_h = 20$  strengthened with steel angles exhibited significantly reduced concrete strain development and a substantial increase in strength.

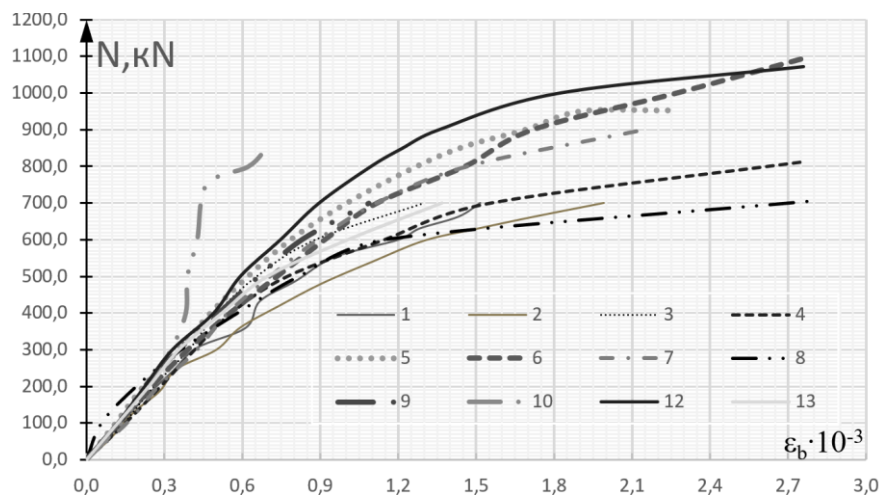


**Fig. 9.** Comparison of average experimental compressive concrete strains in Stage I columns with slenderness  $\lambda_h = 4$  versus applied load, for different hybrid steel-composite strengthening configurations under axial load  $e_0=0$ .

(1- PE<sub>1</sub>; 2-PE<sub>2</sub>; 3- PUM<sub>1</sub>; 4-PUM<sub>1</sub>-X<sub>2</sub><sup>1</sup>; 5-PUM<sub>1</sub>-X<sub>1</sub><sup>2</sup>; 6-PUM<sub>1</sub>-X<sub>2</sub><sup>2</sup>; 7-PUM<sub>1</sub>-X<sub>2</sub><sup>2</sup>H<sup>2</sup>; 8-PUM<sub>2</sub>-X<sub>1</sub><sup>1</sup>; 9-PUM<sub>2</sub>-X<sub>2</sub><sup>1</sup>; 10-PUM<sub>2</sub>-X<sub>3</sub><sup>1</sup>; 11-PUM<sub>2</sub>-X<sub>2</sub><sup>2</sup>; 12-PUM<sub>2</sub>-X<sub>2</sub><sup>2</sup>; 13-PUM<sub>2</sub><sup>2</sup>-X<sub>2</sub><sup>1</sup>)

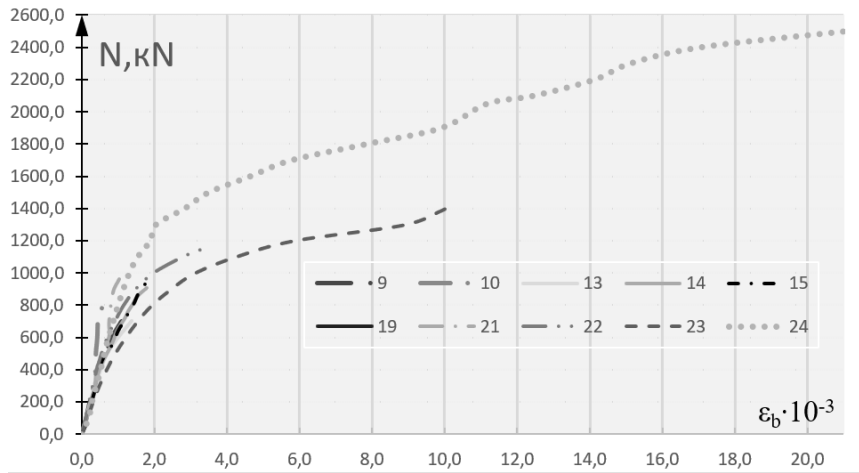


**Fig. 10.** Comparison of average experimental compressive strains of reinforced concrete in Stage I columns with slenderness  $\lambda_h = 4$  versus applied load, for different hybrid steel–composite strengthening configurations under axial eccentricity  $e_0=0$ .

(14-KE<sub>1</sub>; 15-KE<sub>2</sub>; 16-KUM<sub>2</sub>-X<sub>1</sub><sup>2</sup>; 17-KUM<sub>2</sub>-X<sub>2</sub><sup>2</sup>; 18-KUM<sub>1</sub>; 19-KUM<sub>1</sub>-X<sub>1</sub><sup>2</sup>; 20-KUM<sub>1</sub>-X<sub>2</sub><sup>2</sup>).

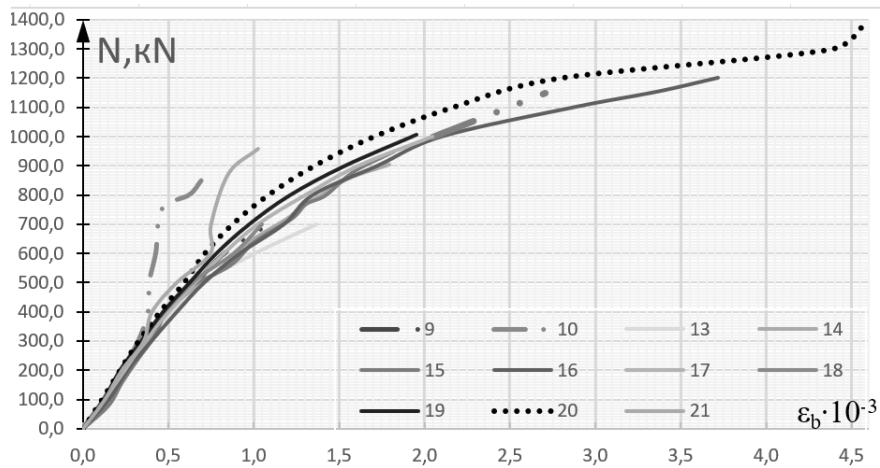


**Fig. 11.** Comparison of average experimental compressive strains of reinforced concrete in columns with slenderness  $\lambda_h = 4$  versus applied load, for different strengthening configurations involving preliminary column rounding, under axial load  $e_0=0$ .

(14-KE<sub>1</sub>; 15-KE<sub>2</sub>; 21-KES; 22-KU; 23-KUN; 24-KUS.)

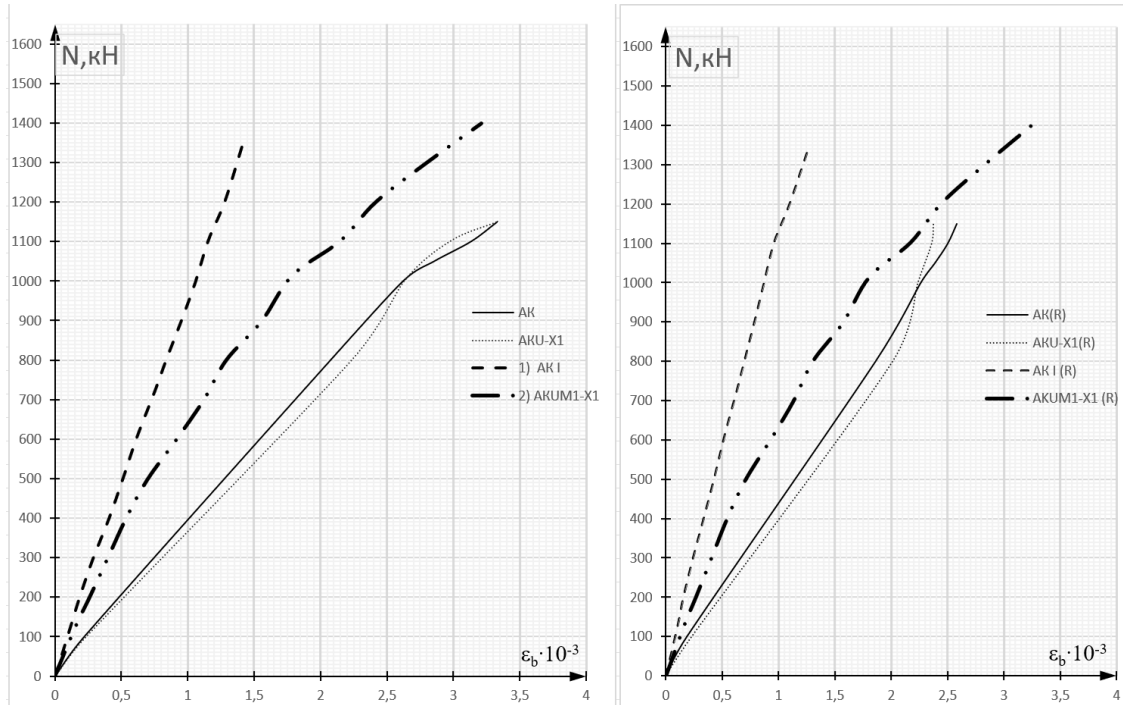


**Fig. 12.** Comparison of average experimental compressive concrete strains –  $\epsilon_{b1}$  and  $\epsilon_{b2}$  on opposite faces of columns ( $\lambda_h = 10$ ) versus applied load, for different strengthening configurations under axial load  $e_0=0$ .

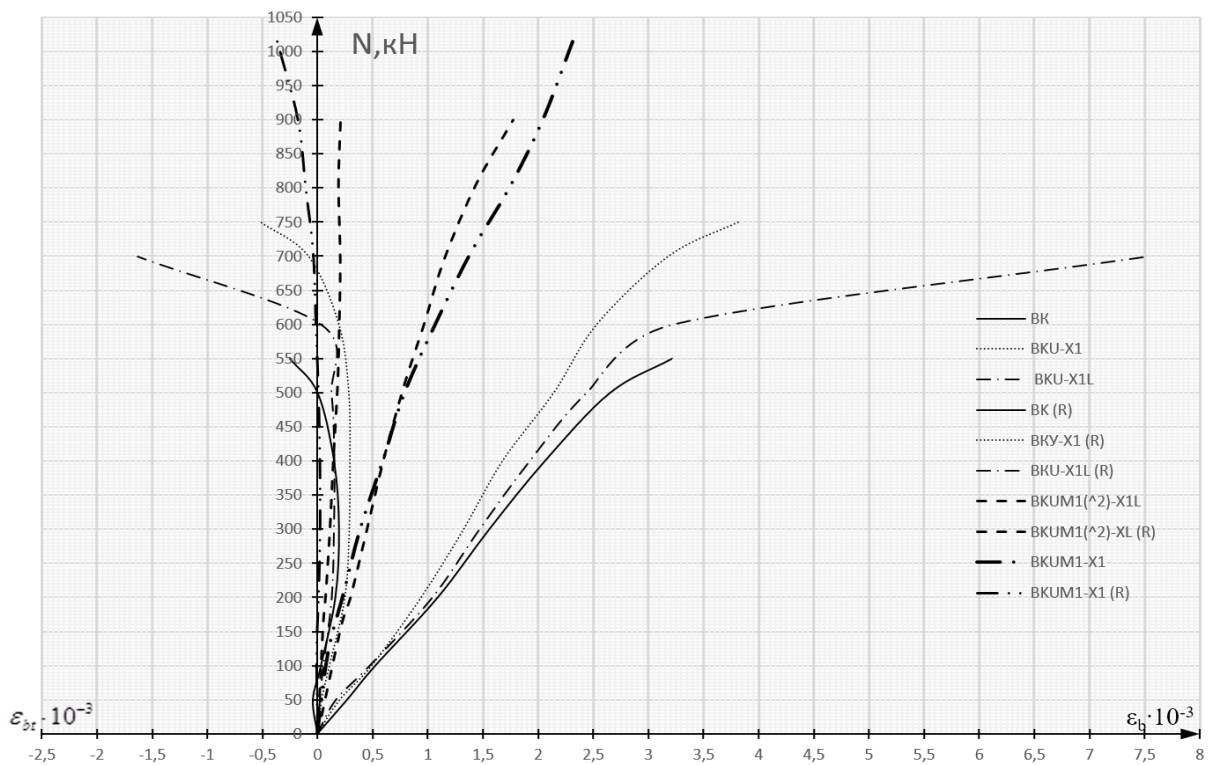


**Fig. 13.** Comparison of average experimental concrete strains in compression–  $\epsilon_b$  and tension –  $\epsilon_{bt}$  on opposite faces of columns ( $\lambda_h = 10$ ) versus applied load, for different strengthening configurations under axial load eccentricity  $e_0 = 2,0 \text{ cm}$  ( $0,16h$ ).

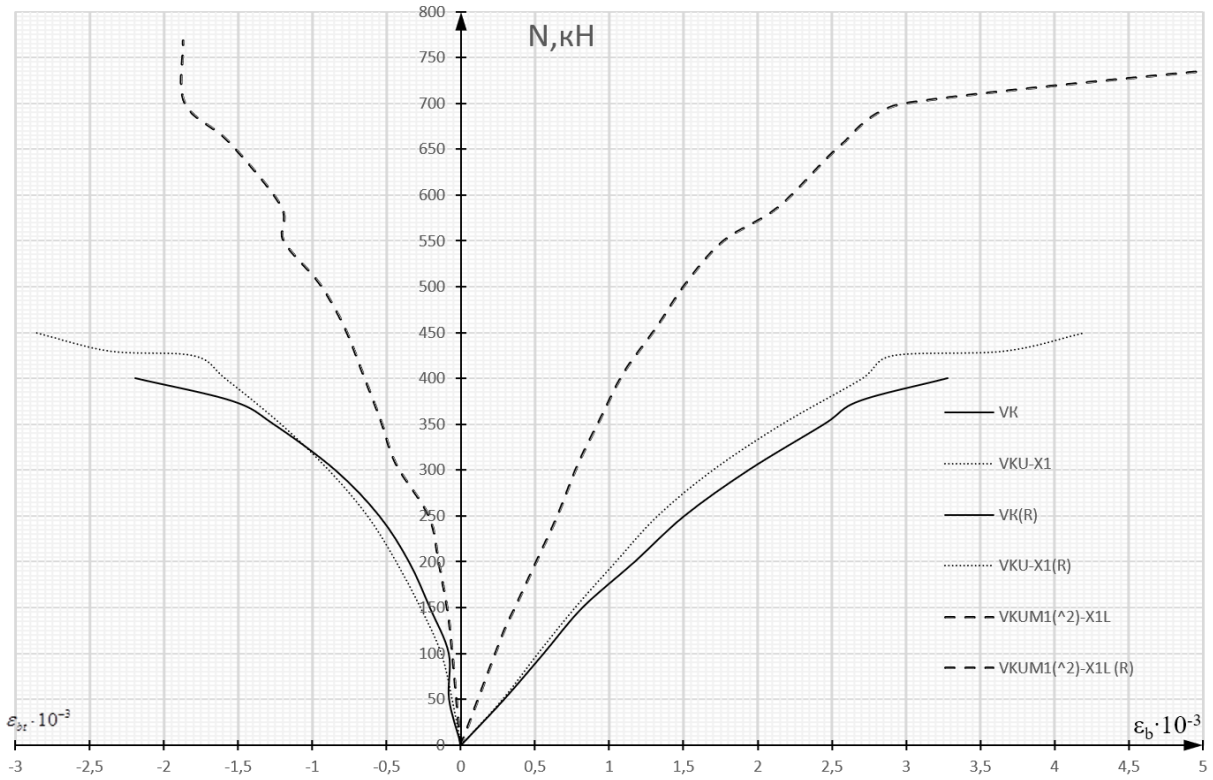


**Fig. 14.** Comparison of average experimental concrete strains in compression –  $\epsilon_b$  and tension –  $\epsilon_{bt}$  on opposite faces of columns ( $\lambda_h = 10$ ) versus applied load, for different composite strengthening configurations under axial load eccentricity  $e_0 = 4,0$  cm (0.32h).

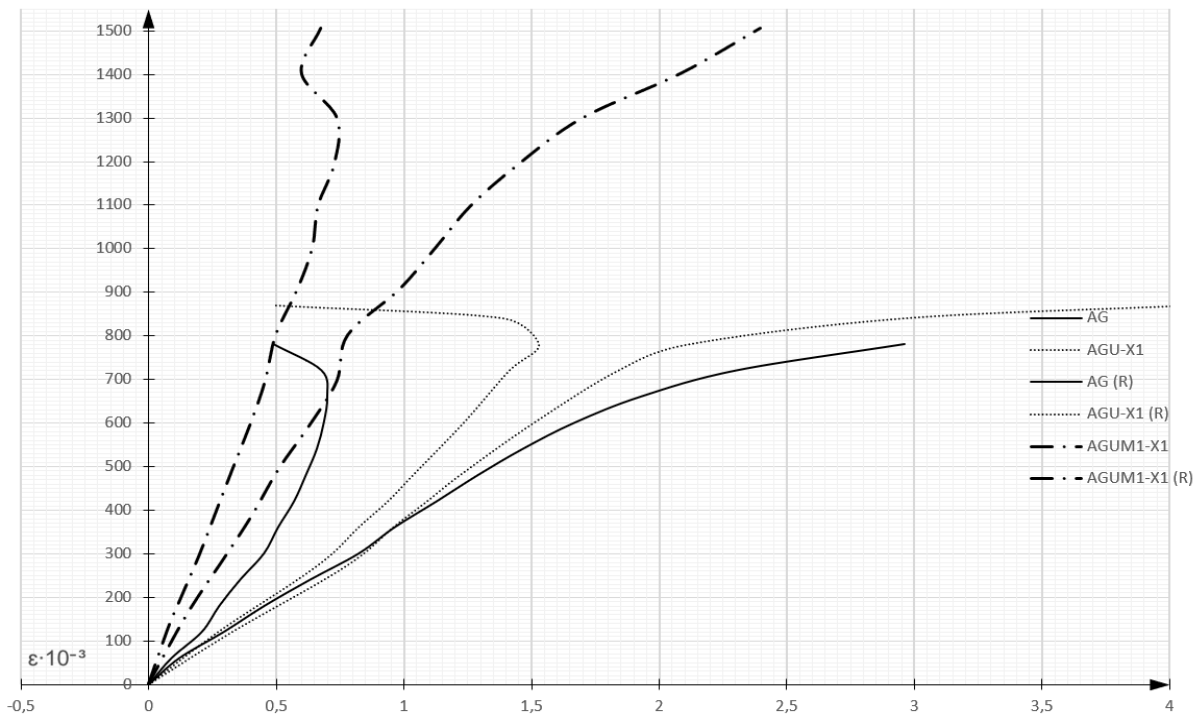


**Fig. 15.** Comparison of average experimental concrete strains in compression–  $\epsilon_b$  and tension–  $\epsilon_{bt}$  on opposite faces of columns ( $\lambda_h = 20$ ) versus applied load, for different strengthening configurations under axial load eccentricity  $e_0 = 0$ .

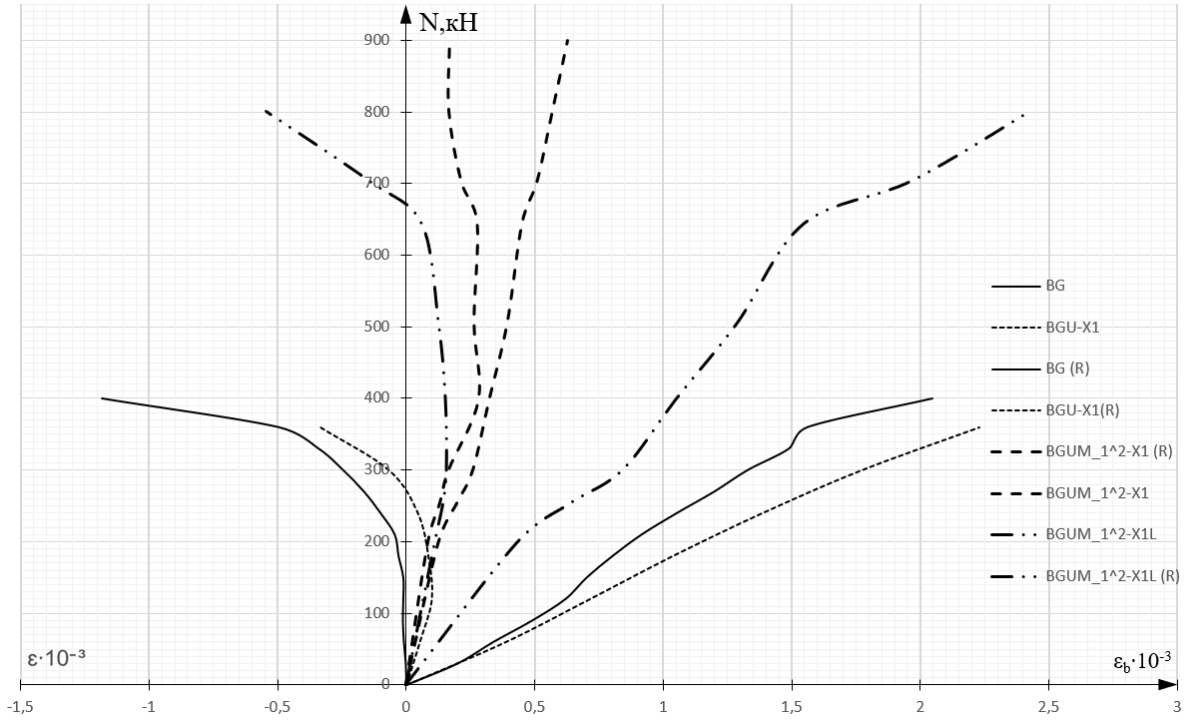


**Fig. 16.** comparison of average experimental concrete strains in compression –  $\varepsilon_b$  and tension –  $\varepsilon_{bt}$  on opposite faces of columns ( $\lambda_h = 20$ ) versus applied load, for different strengthening configurations under axial load eccentricity  $e_0=2,0$  cm (0,16h).

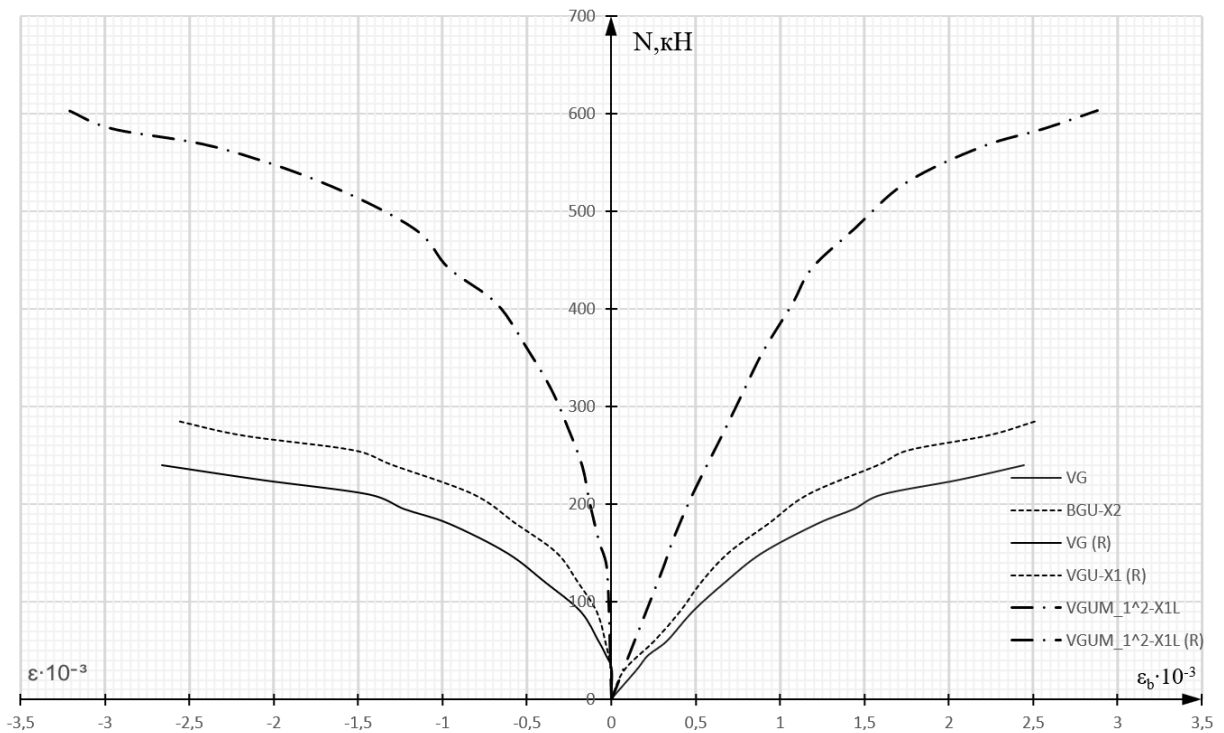


**Fig. 17.** Comparison of average experimental concrete strains in compression –  $\varepsilon_b$  and tension –  $\varepsilon_{bt}$  on opposite faces of columns ( $\lambda_h = 20$ ) versus applied load, for different strengthening configurations under axial load eccentricity  $e_0=4,0$  cm (0,32h).

### Calculation of Load-Carrying Capacity (Theoretical Analysis)

Based on the regulatory documents SP 63.13330 “Concrete and Reinforced Concrete Structures. General Provisions” and SP 164.1325800.2014 “Strengthening of Reinforced Concrete Structures with Composite Materials,” a calculation flowchart was developed (Fig. 18). The flowchart reveals that the current design methodologies specified in the codes do not account for the influence of composite strengthening on the calculated value of concrete’s ultimate compressive strain  $\varepsilon_{b3}$ . Using the experimental values of  $\varepsilon_{b3,exp}$ , obtained during testing (Figs. 9–17), the authors developed proposals for improving the standard design formula for determining  $\varepsilon_{b3}$  (1) by introducing a modification factor  $k_{f1}$ .

To enhance the reliability of  $\varepsilon_{b3}$  prediction, it is proposed to incorporate the factor  $k_{f1}$ , into the formula, which depends on the spacing of the composite hoops and is determined using the newly developed expression (2):

$$\varepsilon_{b3} = \varepsilon_{b2} + k_{f1} \cdot 2 \cdot \mu_f \cdot \frac{R_f}{E_b}, \quad (1)$$

$$k_{f1} = 1,25 \cdot k_\varepsilon - 0,5. \quad (2)$$

Analysis of the obtained strength data for columns with slenderness ratios  $\lambda_h = 10$  and  $\lambda_h = 20$  revealed that, in columns strengthened with transverse composite reinforcement, the concrete compressive resistance  $R_{b3}$ , is influenced by the load eccentricity  $e_0$ . However, current design codes do not account for the effect of eccentricity on  $R_{b3}$  (see Eqs. 3, 4, and 5). Based on the experimental results, a formula for determining the modification factor  $k_{f2}$  (6), has been developed. This factor enables consideration of the load eccentricity  $e_0$  in the evaluation of the enhanced concrete compressive strength  $R_{b3}$  for strengthened columns (7).

$$R_{b3} = R_b + k_{ef} \cdot k_\varepsilon \cdot R_f \cdot \mu_f, \quad \mu_f = A_f/A, \quad (3)$$

$$k_{ef} = 1 - \frac{(b-2r)^2 + (h-2r)^2}{2 \cdot b \cdot h}, \quad (4)$$

$$k_\varepsilon = \left( 1 - \frac{S_w}{2 \cdot (\sqrt{h^2 + b^2} - 2r)} \right)^2, \quad (5)$$

$$k_{f2} = \left( 46,418 \frac{e_0}{h} - 111,43 \left( \frac{e_0}{h} \right)^2 - 0,0142 \right) \cdot e^{\left( 56,131 \left( \frac{e_0}{h} \right)^2 - 25,889 \frac{e_0}{h} + 1,7328 \right) \cdot k_\varepsilon} \quad (6)$$

$$R_{b3} = R_b + k_{f2} \cdot k_{ef} \cdot k_\varepsilon \cdot R_f \cdot \mu_f, \quad (7)$$

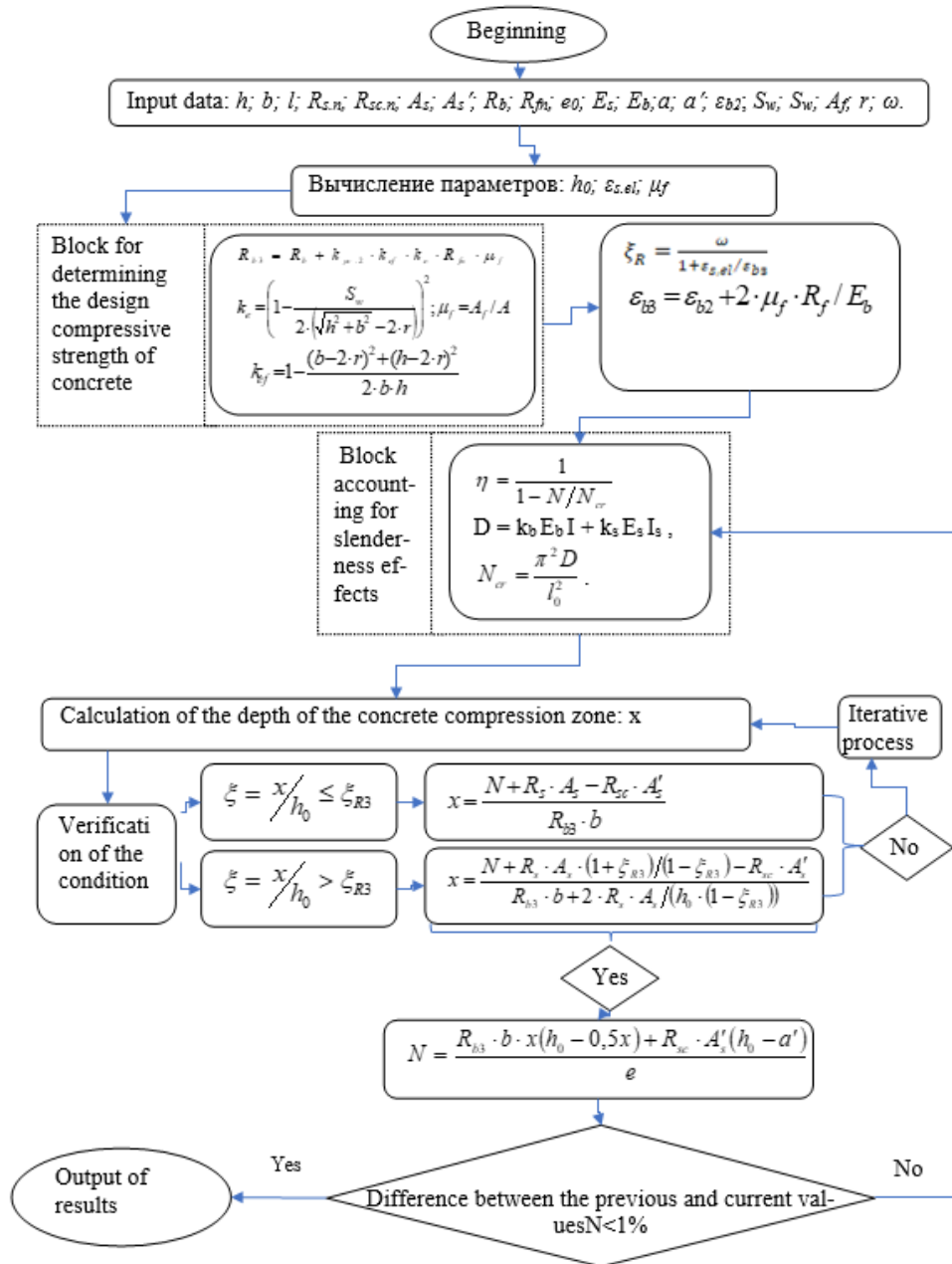


**Fig. 18.** Flowchart for strength calculation of transversely strengthened reinforced concrete columns based on the undeformed configuration.

#### 4. CONCLUSIONS

Based on the conducted research, the following conclusions can be drawn:

- comprehensive experimental investigations of hybrid steel–CFRP-strengthened reinforced concrete columns yielded new data on strength and deformability under variation of key parameters, including column slenderness, load eccentricity, and type/configuration of strengthening.
- the effectiveness of combining steel elements with transversely oriented carbon fiber–reinforced polymer (CFRP) composites has been experimentally confirmed.
- analysis of experimental results demonstrated that bonding steel angles to column corners without transverse composite confinement provides no significant improvement in load-carrying capacity.
- longitudinal strengthening of the concrete compression zone—achieved by externally bonding steel angles—proves particularly effective for slender columns subjected to large load eccentricities.

- hybrid steel–composite strengthening ensures reliable performance throughout all loading stages, with steel, CFRP, concrete, and internal reinforcement acting compositely up to failure.
- steel angles remain securely bonded to the concrete substrate without pull-out; however, their use without transverse CFRP hoops is ineffective.
- strength evaluation confirmed that not only steel angles but also transversely applied CFRP hoops significantly contribute to strength enhancement.
- optimized strengthening configurations were developed for all three load eccentricities ( $e_0 = 0, 2$  cm, and 4 cm), achieving strength increases exceeding 2.5 times that of reference specimens.- test results from 46 columns—including reference and specimens strengthened with various CFRP reinforcement schemes—have enriched the global experimental and analytical database on strengthened concrete members.
- a calculation flowchart for strengthened reinforced concrete members was developed in accordance with current design codes, and proposals were formulated for determining the ultimate compressive strain of strengthened concrete  $\varepsilon_{b3}$  and the enhanced concrete compressive strength  $R_{b3}$ .
- the obtained findings enable identification of key behavioral patterns and will support the development of reliable design methodologies for strengthening concrete and reinforced concrete structures using hybrid steel–composite techniques.

## REFERENCES

1. Kulikova E. Yu., Balovtsev S. V., Skopintseva O. V. Complex estimation of geotechnical risks in mine and underground construction. *Sustainable Development of Mountain Territories*. 2023. 15(1). P. 7-16. DOI: 10.21177/1998-4502-2023-15-1-7-16.
2. Xiao Y, Wu H. Compressive behavior of concrete confined by carbon fiber composite jackets. *Journal of Materials in Civil Engineering*, 2000. 12 (2). P. 144. DOI: 10.1061/(ASCE)0899-1561(2000)12: 2(139)
3. Wu Gang, Lyu Zhitao Study on the stress-strain relationship of FRP-confined concrete circular column without a strain-softening response. *Journal of Building Structures*. 2003. 24 (5). P. 6. DOI: 10.3321/j.issn:1000-6869.2003.05.001
4. Wu Gang, Wu Zhishen, Lyu Zhitao Study on the stress-strain relationship of FRP-confined concrete circular column with a strain- softening response. *China Civil Engineering Journal*, 2006. 39 p.
5. Wu G., Wu Z., Lu Z. Stress-strain relationship for frp-confined concrete prisms. *Fibre-Reinforced Polymer Reinforcement for Concrete Structures*, 2003. P. 561 – 570.
6. Toutanji H, Deng Yong Strength and durability performance of concrete axially loaded members confined with AFRP composite sheets. *Composites: Part B*. 2002. 33 (4). P. 257. DOI: 10.1016/S1359-8368(02)00016-1
7. Youssef M N, Feng M Q, Mosallam A S. Stress-strain model for concrete confined by FRP composites. *Composites: Part B*. 2007. 38 (5/6). P. 623. DOI: 10.1016/j.compositesb. 2006. 07. 020
8. Gu Xianglin, LI Yupeng, Zhang Weiping Compressive stress-strain relationship of concrete confined by carbon fiber composite sheets. *Structural Engineers*. 2006. 22 (2). P. 54. DOI: 10.3969/j.issn.1005-0159.2006.02.012
9. Teng J G, Huang Y L, Lam L. Theoretical model for fiber reinforced polymer confined concrete [J]. *Journal of Composites for Construction*, ASCE. 2007. 11 (2). P. 208. DOI: 10.1061/(ASCE)1090-0268(2007)11:2(201)
10. Klyuyev S.V., Klyuyev A.V., Lesovik R.V., Netrebenko A.V. High strength fiber concrete for industrial and civil engineering. *World Applied Sciences Journal*. 2013. 24(10). P. 1280 – 1285.
11. Abramyan S.G., Klyuev S.V., Polyakov V.G., Sabitova T.A., Akopyan G.O., Guseynov K.M. Specifics of information model development for functional conversion of offshore oil platforms. *Construction Materials and Products*. 2023. 6 (4.) P. 42 – 57. <https://doi.org/10.58224/2618-7183-2023-6-4-42-57>

12. Klyuev S.V., Klyuev A.V., Ayubov N.A., Fediuk R.S., Levkina E.V. Finite Element Design and Analysis of Sustainable Mono-Reinforced and Hybrid-Reinforced Fibergeopolymers. *Advanced Engineering Research (Rostov-on-Don)*. 2025. 25(3). P. 171-185. <https://doi.org/10.23947/2687-1653-2025-25-3-171-185>
13. Wu Gang, Lyu Zhitao. Study on the stress-strain relationship of FRP-confined concrete rectangular columns. *Journal of Building Structures*. 2004. 25 (3). P. 104. DOI: 10.3321/j.issn:1000-6869.2004.03.016
14. Jing Denghu, Cao Shuangyin A model for calculating the axial stress strain curve of square-section concrete column confined by FRP]. *China Civil Engineering Journal*. 2005. 38 (12). P. 35. DOI: 10.3321/j.issn:1000-131X.2005.12.006
15. Pan Jinglong, Wang Yuguang, Lai Wenhui Effect of sectional shape of concrete column on the bearing capacity of short columns wrapped with FRP. *Industrial Construction*, 2001. 31 (6). 18. DOI: 10.3321/j.issn:1000-8993.2001.06.005
16. Kuznetsov D.V., Klyuev S.V., Ryazanov A.N., Sinitsin D.A., Pudovkin A.N., Kobeleva E.V., Nedoseko I.V. Dry mixes on gypsum and mixed bases in the construction of low-rise residential buildings using 3D printing technology. *Construction Materials and Products*. 2023. 6 (6). 5. DOI: 10.58224/2618-7183-2023-6-6-5
17. Abramyan S.G., Klyuev S.V., Emelyanova O.E., Oganesyanyan O.V., Chereshev L.I., Akopyan G.O., Petrosian R.O. Improving reinforced concrete column strengthening techniques for reconstruction projects using composite jacketing formworks. *Construction Materials and Products*. 2023. 6 (5). 1. <https://doi.org/10.58224/2618-7183-2023-6-5-1>
18. Klyuev S.V., Slobodchikova N.A., Saidumov M.S., Abumuslimov A.S., Mezhidov D.A., Khezhev T.A. Application of ash and slag waste from coal combustion in the construction of the earth bed of roads. *Construction Materials and Products*. 2024. 7 (6). 3. <https://doi.org/10.58224/2618-7183-2024-7-6-3>
19. Pukharensko Yu.V., Khrenov G.M., Kluev S.V., Khezhev T.A. Eshanzada S.M. Design of steel fiber-reinforced concrete for slip forming. *Construction Materials and Products*. 2024. 7 (5). 2. <https://doi.org/10.58224/2618-7183-2024-7-5-2>
20. Kachurin N.M., Stas G.V., Prokhorov D.O., Gavrina O.A. Selection of technologies and directions for reducing the technogenic impact of mineral formations on the environment. *Sustainable Development of Mountain Territories*. 2024. 16 (1). P. 283–291. DOI:10.21177/1998-4502-2024-16-1-283-291.
21. Kulikova E.Yu., Balovtsev S.V., Skopintseva O.V. Geoecological monitoring during mining operations. *Sustainable Development of Mountain Territories*. 2024. 16 (2). P. 580–588. <https://doi.org/10.21177/1998-4502-2024-16-2-580-588>.
22. Georgiev S.V., Mailyan D.R, Solovyeva A.I. The high-tech and effective method of strengthening reinforced concrete structures with CFRP materials with preliminary modification of the cross-section shape. *Construction Materials and Products*. 2024. 6 (6). 2. DOI: 10.58224/2618-7183-2023-6-6-2

## INFORMATION ABOUT THE AUTHORS

**Georgiev S.V.**, e-mail: sergey.georgiev@bk.ru, ORCID ID: <https://orcid.org/0000-0001-7278-0948>, SCOPUS: <https://www.scopus.com/authid/detail.uri?authorId=57189056917>, Don State Technical University, Candidate of Engineering Sciences, of the Department of Reinforced Concrete and Stone Structures, Senior Researcher at the Department of Scientific Research

**Mailyan D.R.**, email: dmailyan868@mail.ru, ORCID ID: <https://orcid.org/0000-0002-1175-2078>, SCOPUS: <https://www.scopus.com/authid/detail.uri?authorId=6505969367>, Don State Technical University, Doctor of Engineering Sciences (Advanced Doctor), Professor of the Department of Reinforced Concrete and Stone Structures, Chief Researcher of the Department of Scientific Research

**Solovyeva A.I.**, e-mail: 98rosignol@mail.ru, ORCID ID: <https://orcid.org/0000-0003-2017-7121>, Don State Technical University, Assistant of the Department of Reinforced Concrete and Stone Structures, Junior Researcher at the Department of Scientific Research

**Che Xiang Yu**, e-mail: chexiangyu003@163.com, ORCID ID: <https://orcid.org/0009-0008-4037-4476>, Don State Technical University, Doctoral student, Research assistant in the Don State Technical University laboratory

**Kiiamova L.I.**, e-mail: rostehkazan@mail.ru, ORCID ID: <https://orcid.org/0000-0002-2429-4301>, SCOPUS: <https://www.scopus.com/authid/detail.uri?authorId=58500338500>, National Research Moscow State University of Civil Engineering (NRU MGSU), Department "Construction Technologies and Construction Process Management", Assistant